

**PROGRESS IN THE DEVELOPMENT OF RUGGED LOW POWER COMPACT SILICON MEMS  
SENSORS FOR USE IN NUCLEAR EXPLOSION MONITORING**

Ian M. Standley<sup>1</sup> and W. Thomas Pike<sup>2</sup>

Kinematics Inc.<sup>1</sup> and Imperial College London<sup>2</sup>

Sponsored by Air Force Research Laboratory

Contract No. FA8718-06-C-0011

**ABSTRACT**

In this paper we present the results of our ongoing development of a family of high Q-factor in-plane microelectromechanical systems (MEMS) seismic sensors. We discuss the trade-offs in optimizing the performance for nuclear explosion monitoring. Three different geometries are presented with different optimizations of size versus predicted performance, shock, and vibration resistance. Two of these devices require a vacuum cavity within the device to obtain high Q-factors of the order of ~20,000, while the other device can work with a Q of ~500 that can be obtained in an unsealed cavity. Results of our initial evaluations of the Q obtainable under vacuum are presented showing that Q-factors in excess of 20,000 are obtainable. We also discuss the design and operation of the displacement transducers required for these devices. The transfer of the MEMS fabrication technology from a university to a commercial facility is discussed along with initial fabrication results from a 150mm wafer commercial process, including the formation of vacuum sealed cavities.

**OBJECTIVES**

The objective of this research program is to develop a silicon MEMS sensor suitable for use in Nuclear Explosion Monitoring Systems (NEMS). In Phase A we are developing a triaxial sensor model that we will fabricate and evaluate. This design would then be further optimized in Phase B of the development.

**RESEARCH ACCOMPLISHED**

**Introduction**

Our goal in Phase A of the project has been to complete the design and fabrication of the MEMS component of the sensor optimized for NEMS applications. The MEMS sensor integrates the proof mass and its suspension, a displacement transducer, and a set of electromagnetic transducer coils.

To produce a working microseismometer ( $\mu$ Seis) this MEMS element is coupled with electronic circuitry that excites the displacement transducer, amplifies and demodulates the displacement signal and then feeds back the correct signal to the coils to cause the device to operate as a force-balance acceleration or velocity sensor. Finally, both the MEMS elements and the associated electronics have to be held in a suitable mechanical package to allow the device to operate under field conditions.

**Requirements for NEMs Devices**

For sensing Nuclear Explosions it has been suggested that the noise performance in the band from 10 Hz to 40 Hz is of considerable interest. This band has normally been ignored by broad band sensors which tend to cross the low noise model at approximately 10 Hz. In fact, even the New Low Noise Model (NLNM) is not specified at higher frequencies and in the graph below we have just extrapolated the value from those at ~10Hz. At most sites cultural noise is a significant problem at these frequencies. This is discussed in detail in McNamara et al., 2004 and the figure below shows that at higher frequency the noise is above the NLNM and has degraded at even the best sites in the Continental U.S. due to increased cultural activity.

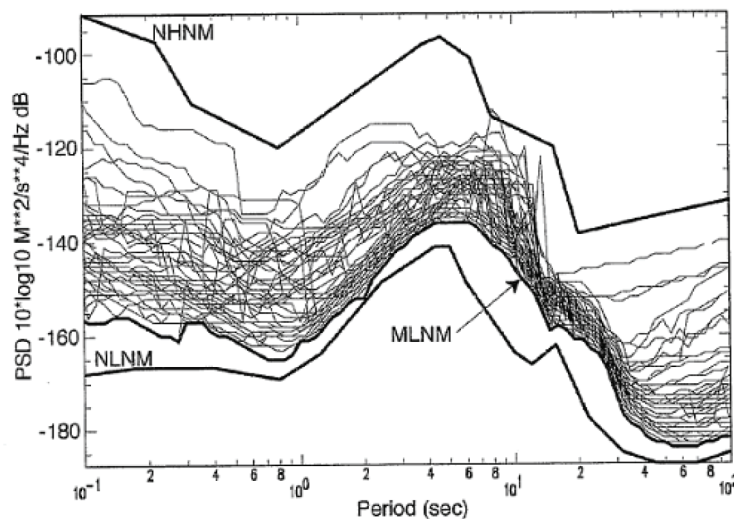


**Figure 1. PDF mode low noise model (MLNM) from McNamara (2004)**

From this figure, we can see that a noise floor of -160dB would resolve the lowest signal level at the vast majority of low noise sites. This level corresponds to ~1 nano-g/ $\sqrt{\text{Hz}}$  in the band of interest. This is the design level that we will use for the microseismometer. Given this requirement our goal was to optimize the design of the MEMS element consistent with the limitations of micro-fabricated devices. A fundamental limit to the performance of a seismometer is given by the Brownian motion of the proof mass itself. The level of this noise is proportional to the square root of the so called “ $MTQ$ ” product of the proof mass and its suspension. Here,  $M$  refers to the mass of the proof mass,  $T$  is the period of the natural frequency of the spring mass system, while  $Q$  is the quality factor of the resonance. For a typical classical broadband sensor using standard mechanics the mass is typically in the order of 200 grams, the

period is several seconds, and Q-factors are of the order of  $\sim 10$ . These values result in an  $MTQ$  product of the order of about unity. For the NEMS application an  $MTQ$  product of  $\sim 0.01$  is required, but with MEMS devices which are batch fabricated from a circular wafer of silicon we are limited to a greatly reduced mass as our die size needs to be limited to about two centimeters square to ensure a reasonable number of devices on a wafer and a reasonable yield of functional parts from those wafers. This results in practical proof masses of the order of 0.25g or almost one thousand times less than a classical broadband instrument.

It would seem that the ideal way to increase the  $MTQ$  product is to just make a very weak suspension with a very large  $T$ . However, while this would work for a horizontal sensor, for a vertical sensor the spring has to balance the earth's gravity and a weak spring would just collapse. Furthermore, in many classical seismometers all the three-axis sensors are tilted: in the so-called Galperin orientation the three sensors are identical and are orientated to lie along the corners of a cube mounted on its corner and each sensor sees about 60% of the earth's gravity. The three axes are recombined electrically to get the vertical and two horizontal components. This Galperin orientation is optimal for a MEMS device as only a single device design is required, rather than separate horizontal and vertical geometries. Thus we need to balance about 0.6 g requiring a spring mass system with a resonance of greater than 10Hz to allow the spring deflection to be accommodated within the dimensions of the device .

Thus, we have lost a factor of 1000 for the mass and an additional factor of  $>10$  for the frequency. For our  $\sim 1$  nano-g/ $\sqrt{\text{Hz}}$  target noise level we are more than a factor of one hundred too low if we were limited to the Q-factor of  $\sim 10$  of mechanical sensors. However, with a MEMS device we can achieve Q-factors of the order of  $\sim 500$  in gas at atmospheric pressure, and over 20,000 in a device sealed in a vacuum allowing us to achieve our required  $MTQ$  product. This explains our interest in MEMS devices for a NEMS sensor as by engineering the Q-factor of the device we can theoretically achieve our required noise floor from a device weighing less than  $\frac{1}{4}$  g in about the area of a postage stamp.

### Device Geometries

After our discussions on the requirements for NEMS devices we altered our original plan and decided to produce three different device geometries. This change was driven by four factors:

1. There is less interest in signals with periods greater than 40 seconds in NEMS sensing, but more interest in extending the high frequency band to 40 Hz.
2. The silicon suspensions had proven fragile and smaller high frequency devices promise to be more robust.
3. Overall package size is an important concern for the final product.
4. The MEMS fabrication house we had selected, IMT, has considerable experience in packaging NEMS devices in sub mtorr vacuum.

The first device is based on our original design with a 20mm x 20mm die size and a natural frequency of 12.5Hz sealed at ambient pressure with a Q-factor of approximately 500. This device includes the changes we had made to improve the shock resistance of the device and the same device is being fabricated at both Imperial College and IMT. This device uses a 200 micron period for the displacement transducer and assumes a spacing of the DT wafer of  $\sim 38$  microns when sealed at ambient pressure.

The second device still utilizes a 20mm x 20mm dies size but increases the natural frequency to a nominal value of 30 Hz, and is designed for vacuum packaging. The higher natural frequency due to the flexure design should further improve the shock and vibration resistance of this device. The design Q-factor is 20,000 which we believe should be obtainable is a vacuum level of  $\sim 0.1$  mTorr and would be dominated by the combination of the intrinsic "Q" of the silicon and the additional damping of the metal interconnects running on the silicon flexures. This device uses a 100-micron period for the displacement transducer and assumes a spacing of the DT wafer of  $\sim 20$  microns when vacuum sealed.

The third device is an experiment to see if a smaller die of 10mm x 10mm that would be configured as an accelerometer could achieve the desired noise floor at higher frequencies using vacuum packaging. The resonant frequency is designed to be 75Hz and the design Q-factor is 20,000. This device uses a 100 micron period for the

displacement transducer and assumes a spacing of the DT wafer of ~ 20 microns when vacuum sealed. The relatively high resonant frequency should result in a rugged and small device.

The design parameters are shown in Table 1, while Figure 2 shows the theoretical suspension noise predicted for each of these devices.

**Table 1. Device Parameters.**

	Die Dimensions	Resonant Frequency /Hz	Design Q-factor	Environment	DT Period / $\mu\text{m}$	Shock Resistance
<b>12.5Hz Device</b>	20mm x 20mm x 0.5mm	12.5Hz	500	Ambient Pressure	200	Moderate
<b>30 Hz Device</b>	20mm x 20mm x 0.5mm	30Hz	20,000	Vacuum ~0.1mTorr	100	High
<b>75 Hz Device</b>	10mm x 10mm x 0.5mm	75Hz	20,000	Vacuum ~0.1mTorr	100	Very High

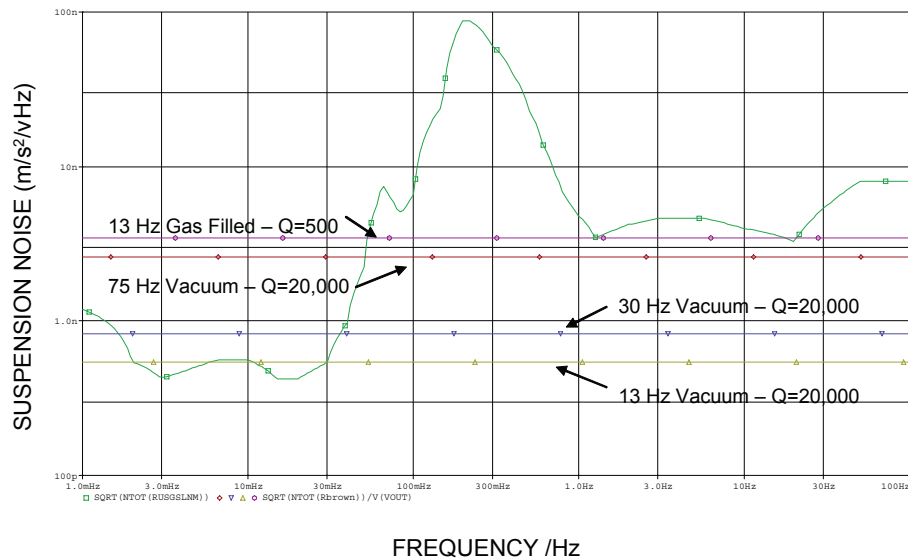


**Figure 2. Predicted suspension noise performance of the various  $\mu\text{Seis}$  geometries related to the NLNM.**

These suspension noise values represent a lower limit to the noise floor of the devices, in reality the actual sensor noise will be determined by other design elements in the electronics. Currently the electronic noise is predicted to be a little lower than the level of the 13Hz gas filled device so the electronics is expected to be the performance limiter for the vacuum sealed devices.

**Quality factor of Micro-Machined Suspensions**

As previously discussed the thermal noise of the microseismometer increases with the damping of the suspension. Damping in these suspensions is a sum of materials damping in the spring itself and gas damping, which at atmospheric pressures is dominated by viscous forces and is independent of pressure. The materials damping, which will dominate at very low pressures, will consist of damping in the silicon itself, expected to be very small, and losses in the surface layers resulting from the deep reactive-ion etching (DRIE) process together with losses in the

metallization of traces along the springs, potentially a much larger contribution (Figure 3). In between the high and low pressure regimes the damping will be pressure dependent, varying in proportion to the viscosity and as the root of pressure.

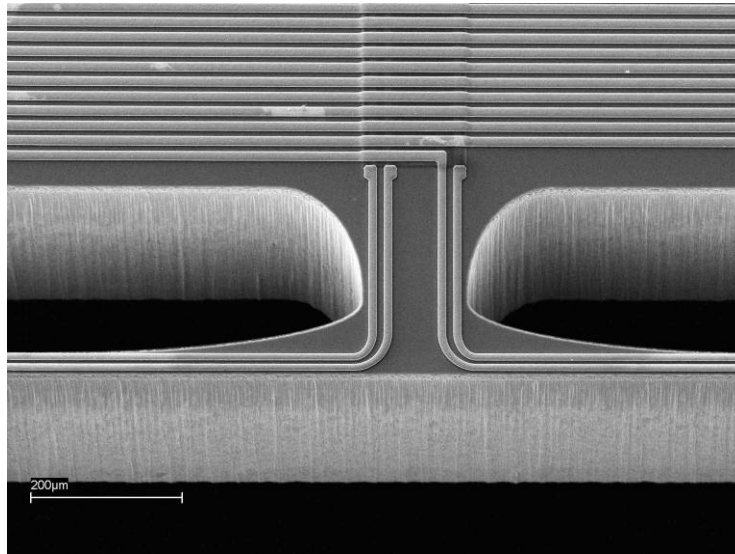


**Figure 3. Part of the micromachined suspension showing sidewall damage and trace metallization that will both contribute to the overall damping.**

The Q factor of the suspensions for the microseismometer has been investigated as a function of pressure, metallization and geometry to quantify the relative contributions of the energy-loss mechanisms (Pike and Standley, 2005). Figure 4 shows a plot of the variation of Q-factor with pressure, as determined by ring-down experiments in air using an optical microscope, or at reduced pressure in an environmental scanning electron microscope. The three regimes are evident and show that low-pressure packaging has the potential of increasing the Q by 500, which would reduce the suspension noise by a little over twenty times.

At the low-pressure limit the Q-factor was found to vary by a factor of two within nominally identical unmetallized suspensions, with the difference attributed to the position of the suspension die within the wafer – it is well known in DRIE that the quality of etching does vary both as a function of distance from the centre of the wafer, and across the wafer with orientation with respect to the gas flow (Chen et al., 2002). In comparison the presence of metallization did not produce a discernible drop in the Q factor. This is most likely due to the very low relative cross section of the metal traces, just  $2 \times 10^{-3}$  of the silicon beam.

In our initial work, the suspension geometry had a more marked effect. Q-factors of the order of about 100,000 were regularly seen in 15 Hz suspensions micro-machined in 20-mm dies, while 75-Hz suspensions on 10-mm dies had a Q-factor more than ten times lower ( $<10,000$ ). This was a concern that vacuum encapsulation would only provide a significant improvement in lower resonant-frequency suspensions. However, some recent results where we used a special process to clean the wafers after DRIE resulted in Q-factors of greater than 50,000 for the 75 Hz suspensions on the 10mm square dies leading us to believe that we can get high Q-factors in the smaller devices which was very encouraging.

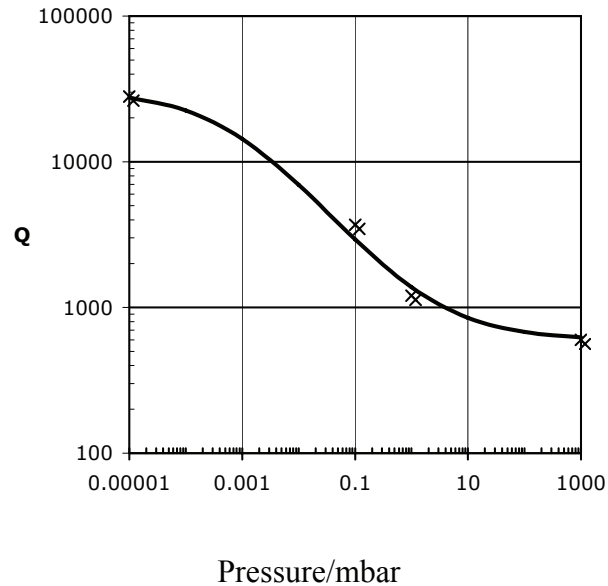


**Figure 4. Q factor as a function of pressure**

### Displacement Transducer

The displacement sensor for the microseismometer is a linear capacitive array transducer (LCAT). The LCAT concept is based on displacement transducer techniques originally developed for conventionally scaled instrumentation, for instance, calipers and linear motion sensors (Baxter and Buehler, 1986; Zhu et al., 1991). The transducer consists of two parallel planes of periodic electrode arrays for drive and pickup (Figure 5). The spacing between the two sets of plates is  $d$ , and the period of the LCAT  $p$ . The strength of the capacitive coupling due to the overlap between drive and pickup electrodes varies periodically with the lateral offset between the two planes. In the  $\mu$ Seis transducer the drive electrodes are driven with out-of-phase voltages, and two sets of pick-up electrodes provide a differential output signal. The capacitive coupling from the positive and negative drives to the corresponding pickup electrodes is given by  $C_{pos}$  and  $C_{neg}$ . At the operating point the displacement sensitivity is a maximum and  $C_{pos} \simeq C_{neg}$ . Stray cross-couplings, summing to  $C_{int}$  will attenuate the output due to the resulting capacitive divider with the transducer capacitance. External capacitance  $C_{ext}$  will provide further attenuation. Optimization of the LCAT consists of determining the transducer geometry that produces maximum displacement sensitivity.

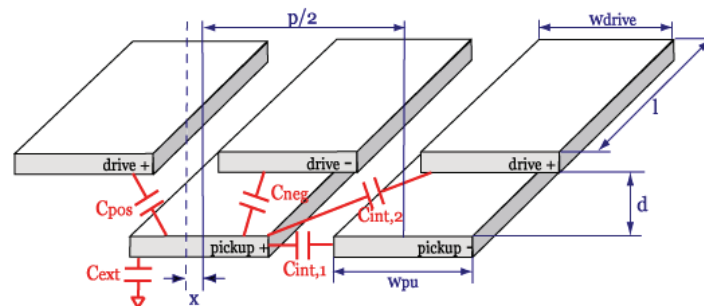


**Figure 5. Diagram of a portion of the differential LCAT geometry.**

This optimization is demonstrated for a mechanical prototype of the microseismometer. There is an optimal  $d/p$  that decreases as the  $C_{ext}/C_{tran}$  decreases. The mechanical microseismometer's calculated optimal sensitivity (normalized to a 1V drive) is 294 V/m at  $w_{pu}/p = 0.45$ ,  $w_{drive}/p = 0.5$ . The experimental sensitivity is 276 V/m and a comparison between the calculated and measured periodic responses is shown in Figure 7. Looking at Figure 6, we see that the sensitivity is well maintained for small deviations from the optimum. For very large strays ( $C_{ext}/C_{tran} > 10$ ), the

optimum  $d/p$  asymptotically approaches 0.3. This method of optimization allows designs to be visualized intuitively with respect to the optimization domains and has been successfully applied to the microseismometer design.

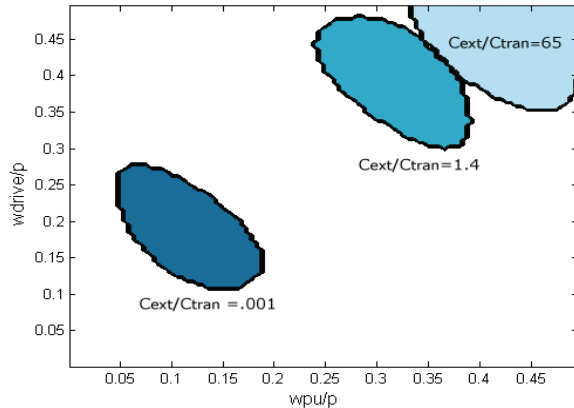


**Figure 6. Domains delineating the electrode geometries producing sensitivities within 3% of optimum for scaled large (as observed), medium and small external capacitances**

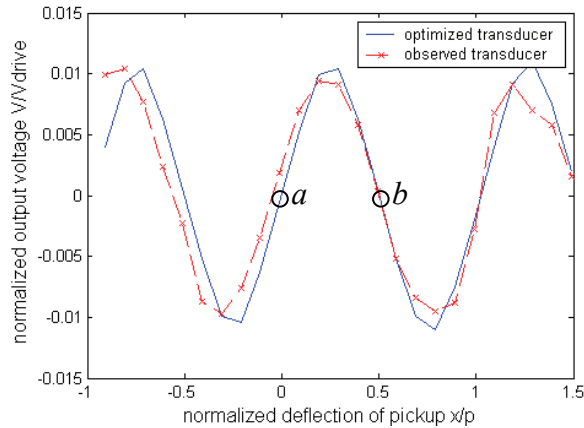


**Figure 7. LCAT output voltage as a function of displacement for the optimized and observed transducers. The feedback points selected for the transfer functions of Figure 8 are indicated.**

### Feedback Control

In order to linearize the output, maximize the range and produce the required velocity output the microseismometer, incorporates feedback to an actuator stabilize the proof mass, with this actuator signal providing the output to the sensor. As the transducer, the LCAT, has multiple null points it is possible to operate the microseismometer with the proof mass positioned at one of a series of positions separated by half the LCAT period. Adjacent null points require a change in sign of the feedback to maintain stability. Figures 8 and 9 show the transfer function of the  $\mu$ Seis mechanical prototype at two adjacent null points. The differences in the closed-loop resonances are due to the non-linearity of the prototype suspension.

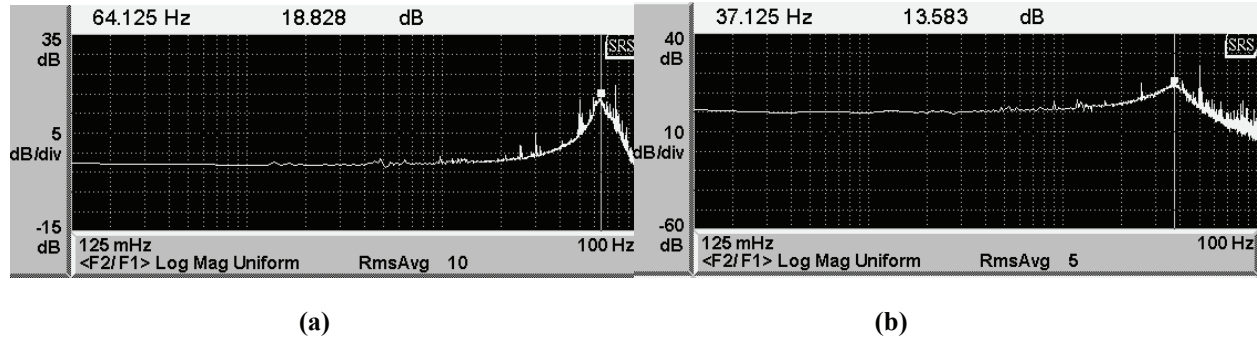


**Figure 8. Closed loop transfer functions of the prototype microseismometer suspension taken at the adjacent operating points of Figure 5. The feedback gain is inverted between the points.**

Operation of the microseismometer is normally closed loop, but the feedback actuation force is limited to displacements just a little larger than one period of the LCAT. As the force limit is reached, a comparator resets the feedback, opening the loop for at least one period of the suspension during which the proof mass re-centers at the new operating position. To assess the feasibility of the scheme, a simulation (Simulink, Mathworks Inc.) was constructed incorporating the dynamics of the  $\mu$ Seis. The results for a stepped input are shown in Figure 9. The proof mass displaces only slightly for input steps less than the actuator range, the shifts a result of the finite gain of the feedback loop. As the actuation limit is reached, the loop is opened and the motion of the proof mass can be seen as it moves to the next null point. Resets are possible of multiple LCAT periods if a sudden change in the signal occurs.



**Figure 9. Simulation of combined closed and open loop operation of the  $\mu$ Seis in response to a stepped input over a 30s period. The input is in red, the position of the proof mass is in blue, showing operation at displacements of 0, 1 and 3 multiples of the LCAT period.**

The final output of the microseismometer under this operation can therefore be constrained to match the range of the digitizer, maximizing the range of the instrument while minimizing the actuation force, and hence noise re-injected back into the feedback loop.

### Transferring Technology to a Commercial MEMS Facility

The silicon microstructure used in the development has been produced in the fabrication facilities at Imperial College on a 100mm fabrication line designed for prototyping experimental MEMS technology, but not dedicated to being able to produce wafers with the high yield required for successful utilization of a device in a product serving the NEMS community. A large part of our development work in the last 8 months has been taking the process developed at Imperial and translating it to work on a commercial MEMS fabrication line. The company we selected to work with was IMT of Santa Barbara California. IMT was selected as they had experience of DRIE and had the same equipment as Imperial College; they had successfully sealed MEMS devices in a high vacuum, and had experience of producing high conductivity electroplated conductors for use in electromagnetic actuators.

The commercialization of a MEMS device and the transfer of the process developed in a University environment to a commercial facility present some unique challenges. MEMS technology is not standardized, unlike the processes used for integrated circuits, so each university and company has their own suite of developed processes. The net result of this is a process redesign to transition from the research to the commercial environment. Such process redesigns tend to have a cascade effect as changes in one process require other changes to maintain compatibility with the metallurgy or etchants required in later stages. From our experience with this transition it certainly needs to be attempted earlier rather than later in the development program and in future programs we would want to involve the commercial facility as soon as the initial design concepts had been proven. One could ask why not do the whole development in a commercial facility? We believe that the answer is that some tasks are more suited both in development time and expense to a university environment. In particular universities expect to be able to fabricate a broad range of designs in parallel, while commercial companies concentrate on high-yield batch fabrication of a single design. An example of this can be seen in increasing the shock resistance of the design of the microseismometer; at Imperial we tried many different spring configurations on the same wafer iterating our mask designs after testing and using low cost masks to solve this problem. This would have been time consuming and more expensive in a commercial facility with the more expensive and longer lead-time photo-masks and with a workflow dedicated to producing batches of identical wafers.

IMT has run a number of short tests to validate each part of the process before attempting to produce the device wafers. This technique has been very valuable as it highlights areas of difficulty and allows them to be resolved on wafers with minimal processing rather than sacrificing wafers with many layers of processing on untested processes.

One of the major challenges was not expected. The DRIE equipment used at both Imperial and IMT is the same model and hence we expected a fairly easy transition of this process that had taken considerable initial development time at Imperial. Although the equipment was the same model the wafer hold down mechanism for the 100mm wafers used at Imperial was different to the 150mm wafer used at IMT. As the DRIE stage releases the proof mass we were finding at IMT that the proof mass and springs would release from the carrier stage and be subject to footing damage. This took considerable process development to overcome. Initially the Q-factors obtained at IMT were variable and lower than obtained at Imperial, but by developing a special cleaning process we have now demonstrated Q-factors of  $\sim 100,000$  in vacuum for the  $\mu\text{Seis}$  12.5Hz device. This is very encouraging, as it exceeds our design goal. Our previous experience suggests that the metal traces will not degrade this number significantly.

At IMT we have also demonstrated that we can seal a silicon wafer to a glass wafer with the required spacing and maintain a vacuum within the device cavity. Figure 10 shows a vacuum sealed wafer and several other electron micrographs of the DRIE and the wafer metallization. Note in the vacuum sealed wafers the black dot in the center and the interference fringes where the wafers have been pushed together by atmospheric pressure and are touching in the center. The DRIE wafer shows a quadrant of the device with the proof mass visible at the top and the three flexure supports and intermediate frames visible below. The final electron micrograph shows two electroplated conductors passing over the edge of the insulating layer.

We are now processing the production wafers at IMT using the processes developed in the short tests discussed above; the wafers are currently waiting for the final metallization before the DRIE etch.

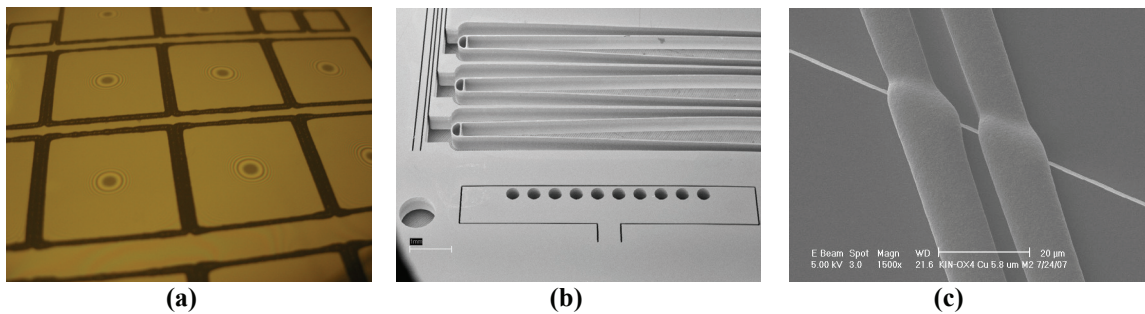


**Figure 10. (a) A sealed test wafer showing the deflection of the areas in the center of the die by the pressure differential. (b) A test wafer after DRIE showing the springs and proof mass. (c) A test wafer showing the conductors passing over the insulator step.**

### CONCLUSIONS AND RECOMMENDATIONS

In our work to date we have demonstrated that we can produce MEMS devices with relatively low natural frequencies compared with previous accelerometers and with very high Q-factors especially when we utilize vacuum sealing. The *MTQ* product of these devices would ensure a suspension noise floor suitable for use in a NEMS sensor. We have also developed a displacement transducer (LCAT) that offers very good performance and coupled with the electro-magnetic coils on the device forms the elements required for a velocity feedback seismometer. We have transferred the majority of the processes required for the fabrication of the microseismometer sensors to a commercial fabrication facility and have shown we can vacuum seal devices. We are now in the process of fabricating completed devices. We will then test the performance of the individual components and then integrate the devices with the mechanics and circuitry to test as a seismometer.

If this testing is successful we would recommend additional work on optimizing both the MEMS element and the electronics to both increase performance and reduce size. Future work aimed at integrating a digitizer into this package may result in a very useful device for NEMS use.

### ACKNOWLEDGEMENTS

We would like to thank the teams at Imperial and Kinometrics who aided the authors in the design, fabrication and testing of the devices: Sunil Kumar, Sanjay Vijendran, Werner Karl Trevor Semple, John Stagg, and Ireck Briones. The team at IMT Inc, of Santa Barbara, California, led by Ian Johnston modified the process and performed the fabrication of the commercial devices.

### REFERENCES

- Baxter, L. K., and R.J. Buehler (1986). United States Patent, No. 4,486,250.
- Chen, K. S., A. A. Ayon, X. Zhang X, and S. M. Spearing (2002) Effect of process parameters on the surface morphology and mechanical performance of silicon structures after deep reactive ion etching (DRIE) *J. Microelectromechanical Systems* 11: 264, 275
- Pike, W. T. and I. M. Standley (2005) Determination of the dynamics of micromachined lateral suspensions in the scanning electron microscope, *J. Micromechanics and Microengineering* 15: S82, S88
- Zhu, F., J. W. Spronck a, and W. C. Heerens (1991). A Simple Capacitive Displacement Sensor *Sensors And Actuators A-Physical* 26: 265, 269.